Adaptive Recovery of a Chirped Signal Using the RLS Algorithm

Paul C. Wei, *Member, IEEE*, James R. Zeidler, *Fellow, IEEE* and Walter H. Ku, *Member, IEEE*

***Abstract*—This paper studies the performance of the recursive least squares (RLS) algorithm in the presence of a general chirped signal and additive white noise. The chirped signal, which is a moving average (MA) signal deterministically shifted in frequency at rate ψ, can be used to model a frequency shift in a received signal. General expressions for the optimum Wiener–Hopf coefficients, one-step recovery and estimation errors, noise and lag misadjustments, and the optimum adaptation constant (β_{opt}) are found in terms of the parameters of the stationary MA signal. The output misadjustment is shown to be composed of a noise ($\xi_0 M\beta/2$) and lag term ($\kappa/(\beta^2\psi^2)$), and the optimum adaptation constant is proportional to the chirp rate as $\psi^{2/3}$.**

The special case of a chirped first-order autoregressive (AR1) process with correlation (α) is used to illustrate the effect the bandwidth ($1/\alpha$) of the chirped signal on the adaptation parameters. It is shown that unlike for the chirped tone, where the β_{opt} increases with the filter length (M), the adaptation constant reaches a maximum for M near the inverse of the signal correlation $(1/\alpha)$. Furthermore, there is an optimum filter length for tracking the chirped signal and this length is less than $(1/\alpha)$.

I. Introduction

ADAPTIVE filters have been extensively studied for diverse applications including adaptive equalization, adaptive prediction, channel estimation, and interference suppression in a variety of stationary environments. For nonstationary environments, two different classes of inputs have been studied for adaptive filtering algorithms. It has been shown that the optimum Wiener solution has a time-varying characteristic that enables the filter to track the minimum point of the error performance surface. In contrast to adaptive filter convergence, which is a transient phenomenon, the tracking characteristics of an adaptive filter are shown to be a steady-state property of the filter. Consequently, good convergence properties do not ensure good tracking performance, and a compromise between the two properties are required for applications in a nonstationary environment [1].

The first class of nonstationary environments considered in [1] arises when the frame of reference provided by the desired response is time varying. This situation occurs in system identification applications when an adaptive transversal filter is used to model a time-varying system. In this case, the correlation matrix of the adaptive filter input is time invariant, but the cross-correlation vector between the filter input and the desired response is time varying. This problem has been analyzed in detail for the case where the unknown dynamic system is modeled as a transversal filter with a time-varying impulse response that is described by a first-order Markov process [1]–[4]. This problem was also analyzed using a frequency domain analysis by Lin *et al*. [5] for the condition that the optimum filter weights have a known power spectrum. This approach is useful when the statistics of the model are known, such as cases where the Jakes model is used to characterize the fading statistics of a communications channel.

The second class of nonstationary environments that has been analyzed in detail consists of a nonstationary stochastic input to the adaptive filter [1]. This situation arises when an adaptive filter is tracking a signal with a time-varying power spectrum for channel equalization, interference suppression, or other applications. This case is more complex to analyze because both the input correlation matrix and the cross-correlation vector are time varying. This class of nonstationarities has only been analyzed for the adaptive predictor application where the input signal consists of a chirped sinusoid in white noise [1], [6]–[10]. These results define how the algorithm performance is determined by the signal parameters.

It was shown in [7] and [8] that there exist optimal adaptation parameters μ (LMS) and β (RLS), which minimize the mean square prediction error for a particular chirp rate and that the improved convergence performance of the RLS over the LMS for stationary inputs does not translate into improved tracking performance for the chirped signal [9]. It was shown by Haykin *et al*. [6] how the unknown signal parameters can be estimated directly from the data and used to improve performance. The advantages of the extended-RLS over the exponentially windowed RLS for this application are discussed in [6]. For lattice implementations, the PARCOR coefficients for the deterministic chirp have been determined analytically for the stochastic gradient lattice and the RLS lattice [10], [11]. It was shown that with the proper choice of the adaptation parameter, the error in the weights can be reduced to a negligible level, within a range of β, which becomes increasingly restrictive as the chirp rate is increased.

This work extends the previous studies for the chirped tone to the more general chirped signal with a defined power

Manuscript received October 4, 1994; revised May 13, 1996. This work was supported by the NSF I/UC Research Center on Ultra High Speed Integrated Circuits and Systems (ICAS), University of California, San Diego, the Office of Naval Research and the National Science Foundation under grant ECD89-16669, and the U.S. Naval Ocean Systems Center Independent Research Program.

P. Wei and W. H. Ku are with the Department of Electrical and Computer Engineering, University of California, San Diego, La Jolla, CA 92093-0407 USA.

J. R. Zeidler is with the Naval Command, Control, and Ocean Surveillance Center, RDT&E Division, San Diego, CA 92152-5000 USA.

Publisher Item Identifier S 1053-587X(97)01170-7.

spectrum. The importance of having a nonzero bandwidth signal is that it more closely resembles a communications signals and other more realistic signals since a zero bandwidth signal is *deterministic* and contains no information. In this paper, the comparative performance for the RLS filter is obtained analytically for a stationary and chirped input signal. The correspondence between the stationary input and chirped input results of the RLS adaptive filter are shown to be related by a chirp matrix and a signal direction vector. These two components define the time-varying properties of the power spectrum.

It is shown that for a chirped first order auto-regressive (AR1) signal, the optimum adaptation constant β_{opt} increases with the filter length (M) until it reaches a maximum for M near the inverse of the signal correlation length $(1/\alpha)$, rather than increasing linearly with the filter length as occurs for the chirped tone. Furthermore, in addition to an optimum adaptation constant, there is also an optimum filter length for tracking the chirped signal, and this length is less than $(1/\alpha)$. This indicates that in nonstationary environments, the reduced correlation between the signal at the end of the filter with the current input signal results in a shorter optimal filter length. The analytical results obtained for the AR1 signal model are shown via simulation to describe the tracking performance of the RLS filter for a BPSK input signal.

In Section II, the signal model is defined, which extends the chirped tone from [7] to the chirped signal considered here. In Section III, the optimum Wiener filter weights for the chirped signal input are derived and related to the optimum weights for the stationary signal. The filter decomposition used to derive RLS tracking performance is summarized in Section IV. This decomposition is then applied to the case of the chirped signal where the elements of the signal correlation must be kept throughout the derivation. In Section V, the noise and lag misadjustments are derived, and the differences between the chirp input nonstationarity (class II) and the filter weight nonstationarity (class I) are discussed. This illustrates the difference between the Markov filter weight model and the results obtained here. The optimum adaptation constant (β_{opt}) is derived in Section VI. In Section VII, analytical results are obtained for a chirped AR1 process, which can be used to model a narrowband communications signal. Finally, in Section VIII, simulations are performed to compare the performance of the RLS for a chirped AR1 process and a BPSK signal. It is shown that for $\beta > \beta_{opt}$, the prediction error is dominated by the stationary filter error components and for $\beta < \beta_{opt}$, the prediction error is dominated by the tracking error.

II. Preliminaries

Consider a stationary baseband communications signal modeled by a moving average (MA) process

$$s_k = \sqrt{P_s} \sum_{l=-\infty}^{k} a_{k-l} u_l \tag{1}$$

where $\{u_l\}$ is a unit variance white noise process, and the $\{a_i\}$ are the MA coefficients. The order-M covariance matrix of a signal vector $\overline{s} = [s_{k-1}, \cdots, s_{k-M}]$ is given by

$$\mathbf{\Phi}^s = P_s \mathbf{R} \tag{2}$$

where $\mathbf{R} = E[\overline{s}^* \overline{s}^T]/P_s$ is the covariance matrix normalized by the signal power (P_s). The elements of $\mathbf{R}$ are given by $(\mathbf{R})_{i,j} = r_{i-j}$, where

$$r_n = \sum_{l=0}^{\infty} a_l a_{l+n}. \tag{3}$$

is the normalized autocorrelation function of the stationary MA signal.

In a nonstationary mobile communication environment, the signal spectrum may be frequency offset and shifted with time. Using this representation, the signal can be frequency shifted and chirped by multiplying each term by a time dependent frequency shift and chirp term to give

$$s_k = \sqrt{P_s} \sum_{l=-\infty}^{k} a_{k-l} \Omega^{k-l} \Psi^{(k^2-l^2)/2} u_l \tag{4}$$

where $\Omega = e^{j\omega}$ defines the initial center frequency of the spectrum, and $\Psi = e^{j\psi}$ linearly shifts the center frequency with time. This simplifies to the deterministic chirp [7] when the stationary signal is a constant DC signal (i.e., $a_k = 1$, and $u_l = \delta_l$), and (4) reduces to

$$s_k = \sqrt{P_s} \Omega^k \Psi^{k^2/2}. \tag{5}$$

The signal correlation $\mathbf{\Phi}_k^s$ is

$$\begin{aligned} E[s_k^* s_{k-m}] &= \sum_{i=-\infty}^{k} \sum_{j=-\infty}^{k-m} a_{k-i}^* a_{k-m-j} E[u_i^* u_j] \\ &\quad \cdot \Omega^{(k-m-j)-(k-i)} \Psi^{[(k-m)^2-j^2-(k^2-i^2)]/2} \\ &= r_m (\Omega^{-m} \Psi^{-mk}) \Psi^{m^2/2}. \end{aligned} \tag{6}$$

It is easy to see from (6) that the correlation function of the chirped signal consists of the correlation function of the stationary process multiplied by the terms representing the signal direction and chirp, respectively. Using the *element by element multiplication* operator $\odot$, which is known as the Hadamard product operator, the input signal correlation can be written in matrix notation as

$$\begin{aligned} \mathbf{\Phi}_k^s &= E[\overline{s}_k^* \overline{s}_k^T] \\ &= P_s \mathbf{R} \odot (\mathbf{V}^k \overline{\mathrm{D}}\, \overline{\mathrm{D}}^H \mathbf{V}^{*k}) \end{aligned} \tag{7}$$

where $\overline{s}_k = [s_{k-1}, \cdots, s_{k-M}]^T$ is the input signal vector, and $\mathbf{R}$ is the correlation matrix of the stationary MA process with elements given by $(\mathbf{R})_{i,j} = r_{i-j}$. The matrix $\mathbf{V}$ is the *chirp matrix*, and $\overline{\mathrm{D}}$ is the *signal direction* given by

$$\begin{aligned} \mathbf{V} &= \mathrm{diag}\,(\Psi, \Psi^2, \cdots, \Psi^m) \\ \overline{\mathrm{D}} &= [\Omega \Psi^{-1/2}, \Omega^2 \Psi^{-2^2/2}, \cdots, \Omega^M \Psi^{-M^2/2}]^T. \end{aligned} \tag{8}$$

At the receiver, the signal is given by

$$x_k = s_k + n_k. \tag{9}$$

where $\{n_k\}$ is a white noise process with power P_n. Using $\mathbf{\Phi}_k^s$

from above, the input autocovariance matrix can be written as

$$\mathbf{\Phi}_k^x = P_n \mathbf{V}^k \mathcal{D} \mathbf{V}^{*k} \tag{10}$$

where

$$\mathcal{D} = [\mathbf{I} + \rho \mathbf{R} \odot (\overline{\mathrm{D}}\,\overline{\mathrm{D}}^H)] \tag{11}$$

and $\rho = Ps/Pn$ is the input signal to noise ratio (SNR). For the deterministic chirp, the stationary signal being chirped is a constant DC signal. Thus, setting the elements of the normalized correlation matrix $(\mathbf{R})_{i,j} = 1$ gives the chirped result in [7].

Similarly, defining the cross correlation vector $(\overline{\theta}_k^f)$ for the one-step forward predictor by

$$\overline{\theta}_k^f = E[x_k \overline{x}_k^*] \tag{12}$$

the cross correlation can be written as

$$\overline{\theta}_k^f = P_s \mathbf{V}^k (\overline{r} \odot \overline{\mathrm{D}}) \tag{13}$$

where $\overline{r} = [r_1, r_2, \cdots, r_{M+1}]^T$ (the second column of $\mathbf{R}$) is the normalized one-step cross correlation vector of the stationary process. The deterministic chirp result is obtained when $\overline{r} = [1, \cdots, 1]^T$.

III. Optimum Wiener Weights

In this section, the Wiener–Hopf equations are solved to find the optimum filter. The optimum Wiener weights are found by solving the Wiener–Hopf equations using the definitions of $\mathbf{\Phi}_k^x$ and $\overline{\theta}_k^f$ defined in Section II to give

$$\overline{W}_k^0 = (\mathbf{\Phi}_k^x)^{-1} \overline{\theta}_k^f. \tag{14}$$

Unlike the deterministic chirp, the covariance matrix of the chirped signal $(\mathbf{\Phi}_k^x)$ cannot be easily inverted, as was done in [7]. However, the Wiener weights can be related those of the stationary signal by substituting (10) and (13) into (14) to give

$$\overline{W}_k^0 = \mathbf{V}^k [\overline{W}^0 \odot \overline{\mathrm{D}}] \tag{15}$$

where $\overline{W}^0$ is the Wiener weight vector when the signal is stationary. This can be verified by using the identities in Appendix G. It can be seen that the optimum weights are also related to the input spectrum through the chirp matrix term $(\mathbf{V}^k)$, and thus, the power spectrum of the prediction filter tracks the input spectrum. (An example of the power spectrum produced by the Wiener weights is plotted, at two distinct values of k, in Fig. 8 for a chirped AR1 process.)

The minimum recovery error is

$$\begin{aligned} E[|\eta_k|^2] &= E[|s_k - (\overline{W}_k^0)^T \overline{x}_k|^2] \\ &= \rho P_n [1 - \overline{r}^H \overline{W}^0]. \end{aligned} \tag{16}$$

It follows that the estimation error (ξ_0) is

$$\begin{aligned} \xi_0 &= E[|e_k|^2] \\ &= E[|x_k - (\overline{W}_k^0)^T \overline{x}_k|^2] \\ &= P_n [1 + \rho(1 - \overline{r}^H \overline{W}^0)] \end{aligned} \tag{17}$$

and the output recovery SNR is

$$\begin{aligned} \rho_0 &= \frac{E[|s_k|^2]}{E[|\eta_k|^2]} \\ &= (1 - \overline{r}^H \overline{W}^0)^{-1}. \end{aligned} \tag{18}$$

These results are identical to the case when the signal is stationary. Note that both $E[|\eta_k|^2]$ and $E[|e_k|^2]$ are independent of k and ψ. Thus, the performance of the optimal filter is equivalent for a stationary signal and for the same signal chirped.

With the weights and performance of the optimum filter established, we are ready to begin the analysis for the weights obtained by the RLS algorithm.

IV. Filter Decomposition

Decomposition of the RLS algorithm is required to analyze the contributions of the lag and noise components of the algorithm from the optimum estimation errors. We will use the same decomposition as [7], which we have summarized below. This decomposition separates the filter update into three components:

1) the transient,
2) the mean,
3) the lag components.

The filter output error is then expressed in terms of these three components and examined in steady state.

The RLS algorithm solves for the optimum filter weights using an exponentially weighted estimate of the input autocorrelation and cross correlation. The algorithm estimates the autocorrelation with

$$\mathbf{R}_k = \sum_{i=1}^{k} \lambda^{k-i} \overline{x}_i^* \overline{x}_i^T \tag{19}$$

and the cross correlation with

$$\overline{P}_k = \sum_{i=1}^{k} \lambda^{k-i} \overline{x}_i^* x_k. \tag{20}$$

Finally, the Wiener–Hopf equation is solved using these estimates to find the optimum weights

$$\overline{W}_k = \mathbf{R}_k^{-1} \overline{P}_k. \tag{21}$$

Equivalently, the optimum filter can be expressed in the recursive form

$$\overline{W}_k = \overline{W}_{k-1} + e(k) \mathbf{R}_k^{-1} \overline{x}_k^* \tag{22}$$

where $e(k)$ is the output error

$$e(k) = x_k - \overline{x}_k^T \overline{W}_{k-1}. \tag{23}$$

This error at time k is the *a priori* error, which is calculated using $\overline{W}_{k-1}$. This is the error most commonly generated by recursive filters and provides an easier analysis due to the assumption on the independence of the $\{\overline{x}_i\}$, which makes $\overline{W}_k$ independent of $\overline{x}_k$. For a stationary signal, the *a priori* and *a posteriori* errors are the same since the filter coefficients $\overline{W}_{k-1} = \overline{W}_k$.

The difference between the RLS implementation of the filter and the optimum filter is often measured by the output prediction error. For the optimum Wiener filter, this is

$$e_0(k) = x_k - \overline{x}_k^T \overline{W}_k^0. \tag{24}$$

where the optimum coefficients $\overline{W}_k^0$ are used. Thus, the difference in the output error power is a result of the difference between the filter weights of the optimum filter and the RLS filter

$$\overline{V}_{k-1} = \overline{W}_{k-1} - \overline{W}_k^0. \tag{25}$$

The output error can be rewritten as

$$e(k) = e_0(k) - \overline{V}_{k-1}^T \overline{x}_k, \tag{26}$$

and because of the orthogonality property of the prediction error with the signal [1]

$$E|e(k)|^2 = \xi_0 + \mathcal{M}_k \tag{27}$$

where

$$\mathcal{M}_k = E|\overline{V}_{k-1}^T \overline{x}_k|^2 \tag{28}$$

is the "misadjustment." We shall now introduce several quantities to allow for the recursive calculation of the "misadjustment" filter:

$$\overline{T}_k = \overline{W}_{k+1}^0 - \overline{W}_k^0 \tag{29}$$

and

$$\mathbf{A}_k = \mathbf{I} - \mathbf{R}_k^{-1} \overline{x}_k^* \overline{x}_k^T. \tag{30}$$

This allows the weight difference vector $\overline{V}_k$ to be written recursively as

$$\overline{V}_k = \mathbf{A}_k \overline{V}_{k-1} + \mathbf{R}_k^{-1} \overline{x}_k^* e_0(k) - \overline{T}_k. \tag{31}$$

Now, the RLS filter can be separated in three components: the Wiener ($\overline{W}_k^0$) filter, which produces the minimum prediction error (ξ_0), and the noise and lag misadjustment filters ($\overline{V}_k$), which produces the noise and lag misadjustments. Since $\overline{V}_k$ is a linear function of $\overline{V}_{k-1}$, the misadjustment can be further decomposed into the following:

1) a transient ($\overline{V}_k^t$) to account for the difference between the initial difference between $\overline{W}^0$ and $\overline{W}_{k=0}$,
2) a lag ($\overline{V}_k^l$), which is introduced because of the nonstationary signal,
3) a noise term ($\overline{V}_k^n$).

The decomposition of $\overline{V}_k$ is thus

$$\overline{V}_k = \overline{V}_k^t + \overline{V}_k^l + \overline{V}_k^n \tag{32}$$

where the components are updated using

$$\begin{array}{ll} \overline{V}_k^t = \mathbf{A}_k \overline{V}_{k-1}^t; & \overline{V}_0^t = \overline{V}_0, \\ \overline{V}_k^l = \mathbf{A}_k \overline{V}_{k-1}^l - \overline{T}_k; & \overline{V}_0^l = 0, \\ \overline{V}_k^n = \mathbf{A}_k \overline{V}_{k-1}^n + \mathbf{R}_k^{-1} \overline{x}_k^* e_0(k); & \overline{V}_0^n = 0. \end{array} \tag{33}$$

The lag term ($\overline{V}^l$) consists of a mean lag term Δ_k plus a random fluctuation $\tilde{V}_k$

$$\overline{V}_k^l = \Delta_k + \tilde{V}_k \tag{34}$$

where

$$\Delta_k = E[\overline{V}_k^l]. \tag{35}$$

We will show that the random fluctuation $\tilde{V}_k$ is small under the "slow variation" ($M\psi \ll \beta$) and "slow adaptation" ($\beta M \ll 2$) conditions defined by Macci and Bershad [7]. The explicit expansions of $\overline{V}_k$ can be obtained by noting that $\mathbf{A}_k = \lambda \mathbf{R}_k^{-1} \mathbf{R}_{k-1}$ from the definition of $\mathbf{A}_k$ (30) and $\mathbf{R}_k$ (19). This gives

$$\overline{V}_k^t = \lambda^k \mathbf{R}_k^{-1} \mathbf{R}_0 \overline{V}_0^t, \tag{36}$$

$$\overline{V}_k^l = -\mathbf{R}_k^{-1} \sum_{j=1}^{k} \lambda^{k-j} \mathbf{R}_j \overline{T}_j \tag{37}$$

and

$$\overline{V}_k^n = \mathbf{R}_k^{-1} \sum_{j=1}^{k} \lambda^{k-j} \overline{x}_j^* e_0(j). \tag{38}$$

The transient component ($\overline{V}_k^t$) can be neglected in steady state for $k \gg 1$ since $\lambda^k \to 0$ for large k. Thus, the total misadjustment is

$$\mathcal{M}_k = \mathcal{M}_k^l + \mathcal{M}_k^n \tag{39}$$

where the noise and lag misadjustment are

$$\mathcal{M}_k^{l,n} = E|\overline{x}_k^T \overline{V}_{k-1}^{l,n}|^2. \tag{40}$$

These quantities will reflect the degraded performance and sensitivity of the RLS algorithm to the chirp nonstationarity. In the following section, the noise and lag misadjustments will be derived.

V. Filter Misadjustment

It was previously shown in [7] that for the sinusoidal chirp at time $k \gg 1$, the covariance matrix estimate $\mathbf{R}_k$ is quasideterministic under the assumption of "slow adaptation" ($\beta M \ll 2$) and "slow variation" ($M\psi \ll \beta$), i.e.,

$$E|\mathbf{R}_k - E[\mathbf{R}_k]|^2 \ll |E[\mathbf{R}_k]|^2. \tag{41}$$

In Appendix E, this is also shown to be true for a generalized chirped signal under the above assumptions. This greatly simplifies the analysis, allowing $\mathbf{R}_k$ to be moved outside of the expectation operator. A similar approach was used in [3] to show this property for a general nonstationary input when β is sufficiently small. In the following sections, the noise, the mean lag, and the lag fluctuation misadjustments will be derived using the quasideterministic property of $\mathbf{R}_k$.

A. Noise Misadjustment

First, the noise misadjustment is given by

$$\mathcal{M}_{k+1}^n = E|\overline{x}_{k+1}^T \overline{V}_k^n|^2 \tag{42}$$

where from (38)

$$|\overline{x}_{k+1} \overline{V}_k^n|^2 = \sum_{m,n=1}^{k} \lambda^{2k-m-n} \overline{x}_{k+1}^T \cdot \mathbf{R}_k^{-1} \overline{x}_m^* e_0(m) e_0(n)^* \overline{x}_n^T \mathbf{R}_k^{-1} \overline{x}_{k+1}^*. \tag{43}$$

Assuming that the error $e_0(k)$ is independent of past inputs $\overline{x}_l$, $(l < k)$,[1]

$$\mathcal{M}_{k+1}^n = \sum_{n=1}^{k} \lambda^{2(k-n)} \xi_0 E[\overline{x}_{k+1}^T \mathbf{R}_k^{-1} \overline{x}_n^* \overline{x}_n^T \mathbf{R}_k^{-1} \overline{x}_{k+1}^*] \quad (44)$$

where $\xi_0 = E[e_0^*(m)e_0(n)]$ is the minimum estimation error. Using the trace ($\mathrm{Tr}\{\cdot\}$) allows the rearrangement of the products to give

$$\mathcal{M}_{k+1}^n = \xi_0 \sum_{n=1}^{k} \lambda^{2(k-n)} \mathrm{Tr}\{E[\mathbf{R}_k^{-1} \overline{x}_{k+1}^* \overline{x}_{k+1}^T \mathbf{R}_k^{-1} \overline{x}_n^* \overline{x}_n^T]\}.$$

Finally, after using the approximations on $\mathbf{R}_k$ and λ, it is shown in Appendix B that

$$\mathcal{M}_{k+1}^n = \frac{\beta}{2} M \xi_0 \quad (45)$$

where $\beta = 1 - \lambda$. This is the same form as in the deterministic chirp case [7]. For a chirped nonzero bandwidth signal, ξ_0 will be larger than for a deterministic chirped signal. A derivation of $\mathcal{M}^n$ applicable over a wider range of β can be found in [3], which is given by

$$\mathcal{M}_{k+1}^n = \frac{\beta}{2 - \beta} M \xi_0. \quad (46)$$

For small β, the two forms are nearly identical.

B. Mean Lag Misadjustment

Second, the misadjustment from the mean lag is given by

$$\mathcal{M}_{k+1}^{\Delta} = E|\overline{x}_{k+1}^T \Delta_k|^2 \quad (47)$$

where from (35) and (37)

$$\Delta_k = -\mathbf{R}_k^{-1} \sum_{j=1}^{k} \lambda^{k-j} \mathbf{R}_j T_j. \quad (48)$$

Because of the summation over j, the first order "slow variation" approximation for $\mathbf{R}_j$ cannot be used. In Appendix C, the exact expression is evaluated in steady state ($k \gg 1$) to give

$$\Delta_k = -\frac{P_n}{\beta} \mathbf{R}_k^{-1} \mathbf{V}^{k+1} (\mathbf{V} - \lambda \mathbf{I})^{-1} \cdot (\mathbf{I} + \rho\beta \mathbf{R} \odot \mathbf{H}_1)(\mathbf{V} - \mathbf{I}) \overline{z} \quad (49)$$

where

$$\overline{z} = \rho \mathcal{D}^{-1}(\overline{r} \odot \overline{\mathrm{D}}) = \overline{W}^0 \odot \overline{\mathrm{D}}. \quad (50)$$

The slow variation assumption $M\psi \ll \beta$ implies that

$$[\mathbf{V} - \lambda \mathbf{I}]^{-1} \approx \beta^{-1} \mathbf{I} \quad (51)$$

and from the definition of $\mathbf{H}_1$ (A3)

$$\mathbf{H}_1(\lambda) \approx \beta^{-1} \mathbf{V} \overline{\mathrm{D}}\, \overline{\mathrm{D}}^H \mathbf{V}^*. \quad (52)$$

Thus, we have

$$(\mathbf{I} + \rho\beta \mathbf{R} \odot \mathbf{H}_1) = \mathbf{V} \mathcal{D} \mathbf{V}^*. \quad (53)$$

This reduces Δ_k to

$$\Delta_k = -P_n \mathbf{R}_k^{-1} \frac{\mathbf{V}^{k+1}}{\beta^2} \mathbf{V} \mathcal{D} \mathbf{\Lambda} \overline{z} \quad (54)$$

where $\mathbf{\Lambda} = (\mathbf{I} - \mathbf{V}^*)$. Using the steady-state value of $\mathbf{R}_k^{-1}$ from (A8), the mean weight error due to lag is

$$\Delta_k = -\frac{1}{\beta} \mathbf{V}^{k+1} \mathbf{\Lambda} \overline{z}. \quad (55)$$

Here, we have used the slow variation approximation ($\mathbf{V} \approx \mathbf{I}$) to reduce the term $\mathcal{D}^{-1} \mathbf{V} \mathcal{D} \approx \mathbf{I}$. Thus, the mean lag misadjustment is given by

$$\mathcal{M}_{k+1}^{\Delta} = \frac{P_n}{\beta^2} (\mathbf{\Lambda} \overline{z})^H \mathcal{D} (\mathbf{\Lambda} \overline{z}). \quad (56)$$

This is essentially the same as (4.23) in [7], where, for the deterministic chirp, the term $(\mathbf{V}^* - \mathbf{I}) K \overline{\mathrm{D}}$ corresponds to $-\mathbf{\Lambda} \overline{z}$, the $\mathbf{R}$ inside $\mathcal{D}$ is the matrix of ones, and the approximation $\mathbf{V} \approx \mathbf{I}$ has been applied using the slow variation approximation.

This can be rewritten in terms of the stationary process components ($\overline{W}^0$, $\mathbf{\Phi}^x$) using the matrix relations (G1) and (G2) to give

$$\mathcal{M}_{k+1}^{\Delta} = \frac{1}{\beta^2} (\mathbf{\Lambda} \overline{W}^0)^H \mathbf{\Phi}^x (\mathbf{\Lambda} \overline{W}^0) = \frac{\kappa}{\beta^2} \psi^2 \quad (57)$$

where

$$\kappa = \frac{(\mathbf{\Lambda} \overline{W}^0)^H \mathbf{\Phi}^x (\mathbf{\Lambda} \overline{W}^0)}{\psi^2}, \qquad M\psi \ll \beta \quad (58)$$

is the "*normalized lag misadjustment*"[2] for a chirped process. In addition, since $\mathbf{\Phi}^x$ is a correlation matrix (positive definite), it can be seen that $M_{k+1}^{\Delta} \propto |\overline{W}^0|^2$, i.e., the lag misadjustment is proportional to the magnitude squared of the optimum Wiener weights. It is important to keep this in mind as it will explain much of the behavior of the lag misadjustment. This will have the effect of reducing the lag misadjustment as the filter/signal bandwidth increases and will be illustrated with a chirped AR1 process in Section VII.

C. Lag Fluctuation Misadjustment

Last, the lag misadjustment is derived in [12] and is shown to be

$$\tilde{\mathcal{M}}_{k+1} = \frac{\frac{\kappa}{4\beta} \psi^2 \mathrm{Tr}[(\mathbf{\Phi}^x)^{-1}]}{P_n} = \frac{\kappa}{4\beta} \psi^2 \sum_{i=1}^{M} (1 + \rho\sigma_i^2)^{-1} \leq \frac{M\kappa}{4\beta} \psi^2 \quad (59)$$

[1] This is approximately true when the filter length is sufficiently long to remove most of the signal, thus leaving $e_0(k) \approx n_k$ [7].

[2] The term ψ^2 is isolated because for small ψ the matrix $\mathbf{\Lambda}$ is proportional to ψ.

where $\{\sigma_i\} = eig(\mathbf{R})$ are the eigenvalues of the normalized signal correlation matrix $\mathbf{R}$. The ratio of the fluctuation with respect to the mean lag misadjustment is

$$\begin{aligned}\frac{\tilde{\mathcal{M}}_{k+1}}{\mathcal{M}^{\Delta}_{k+1}} &\leq \frac{\frac{M\kappa}{4\beta}\,\kappa\psi^2}{\frac{\kappa}{\beta^2}\,\psi^2} \\ &\leq \frac{M\beta}{4} \\ &\ll 1 \end{aligned} \tag{60}$$

and can be neglected. This can be compared with the chirp case, where this ratio is given by $(M-1)\beta/4$.[3] Thus, the ratio of fluctuation misadjustment to mean lag misadjustment remains relatively constant when the stationary signal being chirped is changed.

D. Discussion

The lag misadjustment arises from the weight difference between optimum and the RLS filter weights and is proportional to the magnitude of the weight difference vector. In the chirped signal case, the time-variant weights in (15) are seen to obey a first-order Markov difference equation with no white noise forcing term

$$\overline{W}^0_k = \mathbf{V}\overline{W}^0_{k-1}. \tag{61}$$

This is similar to the weight behavior of the tracking model studied in [3] where the weights are given by

$$\overline{W}^0_k = \alpha\overline{W}^0_{k-1} + \overline{n}_k \tag{62}$$

and $\overline{n}$ is a zero mean Gaussian random vector. There, the tracking analysis was performed for $\alpha \approx 1$, where the weight update is dominated by the noise $\overline{n}_k$. At time k, the weight difference is

$$\Delta_k \approx \sum_{m=1}^{k} \lambda^{k-m}\overline{n}_m. \tag{63}$$

Because the updates are white, they *do not sum coherently*, and the squared magnitude of the weight difference vector is approximately $M\sigma_n/2\beta$.

In the chirped signal case defined by (61), the weight updates *sum coherently* to give the difference in (55)

$$\Delta_k \approx -\frac{1}{\beta}\,\mathbf{V}^{k+1}\Lambda\overline{z}.$$

Thus, in this case, the squared magnitude of the weight difference vector is $\overline{z}^H\Lambda^H\Lambda\overline{z}/\beta^2$.

Thus, when the nonstationary weights can be written as a first order Markov model, two cases arise: 1) When weight updates are dominated by the white noise term, the lag misadjustment is of order $1/\beta$, and 2) when weight updates are dominated by previous weight, the lag misadjustment is of order $1/\beta^2$.

[3]The $(M+2)$ term of $\tilde{\mathcal{M}}_{k+1}$ given in [7] should be $(M+1)$ and, thus, the result.

VI. Optimal Adaptation Constant β_{opt}

Using the previous results for the misadjustment, the adaptation parameter β can now be optimized to reduce the filter misadjustment. The total misadjustment is the sum of the noise (45) and lag (57) misadjustments

$$\mathcal{M} = \frac{\beta M}{2}\,\xi_0 + \frac{\psi^2}{\beta^2}\,\kappa. \tag{64}$$

Since the noise and lag components behave oppositely as β is changed, there exists an optimum β that minimizes $\mathcal{M}$. Solving for the minimum with respect to β, the optimum adaptation constant can be shown to be

$$\beta_{opt} = \psi^{2/3}\left(\frac{4\kappa}{M\xi_0}\right)^{1/3}. \tag{65}$$

The parameters of the *stationary* process are contained in the ratio $(\kappa/\xi_0)^{1/3}$, and this ratio is the only quantity that needs to be recalculated when a different signal is chirped. Note that β_{opt} increases with the chirp rate ψ in order to put more emphasis on the current data.

The minimum misadjustment is

$$\mathcal{M}_{\min} = \tfrac{3}{4}\,M\xi_0\beta_{opt}. \tag{66}$$

When $\beta = \beta_{opt}$, the mean lag misadjustment is half of the noise misadjustment. Thus, for a given chirp rate, if $\beta = \beta_{opt}(\psi)$, then the total misadjustment will only increase by a factor of 3/2 from the stationary cases when the signal is chirped at rate ψ.

The "slow variation" assumption on the input is primarily used to derive a manageable solution in the region of interest, i.e., where the filter is able to track well. The interested reader can derive the misadjustments without the slow variation assumption using (A5) for $\mathbf{R}_k$. The simulation results in Section VIII will illustrate that the β_{opt} provided by the "slow variation" assumption is a good choice for the adaptation constant β. In the following section, we apply these results to an AR1 process to illustrate their applicability. The correspondence to the deterministic chirp result is discussed in Appendix D.

VII. Chirped AR1 Process

To illustrate the performance of the RLS algorithm for a chirped nonzero bandwidth signal, these results are applied to a chirped AR1 process. The AR1 process can be used to model many narrowband processes, and in Section VIII, it will be shown that these results provide a reasonable approximation to those of a chirped BPSK input signal. The first-order autoregressive process has the recurrence equation

$$s_k = \alpha s_{k-1} + u_k \tag{67}$$

where u_k is a white noise process, with $\sigma_u^2 = P_s(1-\alpha^2)\delta_{i-j}$. The corresponding moving average coefficients for (1) are

$$a_k = \alpha^k, \qquad k = 0, 1, \cdots \tag{68}$$

and the normalized covariance matrix in (2) is

$$(\mathbf{R})_{i,j} = \alpha^{|i-j|}. \tag{69}$$

In a mobile environment, the baseband signal is modulated for transmission and may be Doppler shifted due to the relative motion between the transmitter and receiver. At the receiver, this frequency-shifted signal can be modeled as a chirped AR1 process with (4) to give

$$s_k = \sum_{l=-\infty}^{k} \alpha^{k-l}\Omega^{k-l}\Psi^{(k^2-l^2)/2}u_l \tag{70}$$

which corresponds to the autoregressive form

$$s_k = \alpha\Omega\Psi^{-1/2}\Psi^k s_{k-1} + u_k. \tag{71}$$

The normalized one step cross-correlation vector of the stationary AR1 process is given by

$$\overline{r} = [\alpha,\, \alpha^2,\, \cdots,\, \alpha^M] \tag{72}$$

and the cross-correlation vector of the chirped signal is found from (13)

$$\overline{\theta}^f = P_s\overline{r} \odot (\mathbf{V}^k\overline{\mathrm{D}}).$$

A sample stationary AR1 process is shown in Fig. 1, and a chirped version of the same signal is shown in Fig. 2. The optimum weights for the stationary AR1 process were studied in [13] for interference suppression applications and are reproduced below for convenience.

$$(\overline{W}^0)_l = B_1 b^l + B_2 b^{M-l}, \qquad l = 1, \cdots, M \tag{73}$$

where b corresponds to the filter bandwidth

$$b = \gamma - \sqrt{\gamma^2 - 1}. \tag{74}$$

The coefficients (B_1, B_2) are given by

$$B_1 = \frac{(\alpha - b)(1 - \alpha b)^2}{b[(1 - \alpha b)^2 - b^{2M}(\alpha - b)^2]},$$
$$B_2 = \frac{b^M(\alpha - b)^2(1 - \alpha b)}{[(1 - \alpha b)^2 - b^{2M}(\alpha - b)^2]} \tag{75}$$

where

$$\gamma = \frac{1}{2\alpha}[(1 + \alpha^2) + \rho(1 - \alpha^2)].$$

The corresponding chirped process has Wiener weights given by

$$\overline{W}_k^0 = \mathbf{V}^k[\,\overline{W}^0 \odot \overline{\mathrm{D}}\,]. \tag{76}$$

It is seen that the transfer function of the optimum filter moves with the input signal spectrum. (A sample Wiener filter power spectrum at two time instants is plotted in Fig. 8 for a chirped AR1 process.)

Because the chirp does not change the performance of the Wiener filter, the output recovery SNR is the same as that of the stationary signal derived in [13], i.e.,

$$\rho_0 = \left[1 - \frac{\alpha(\alpha - b)(1 - \alpha b)(1 - b^{2M})}{(1 - \alpha b)^2 - b^{2M}(\alpha - b)^2}\right]^{-1}. \tag{77}$$

However, unlike the deterministic chirp, the output recovery SNR is bounded as the filter length M is increased.

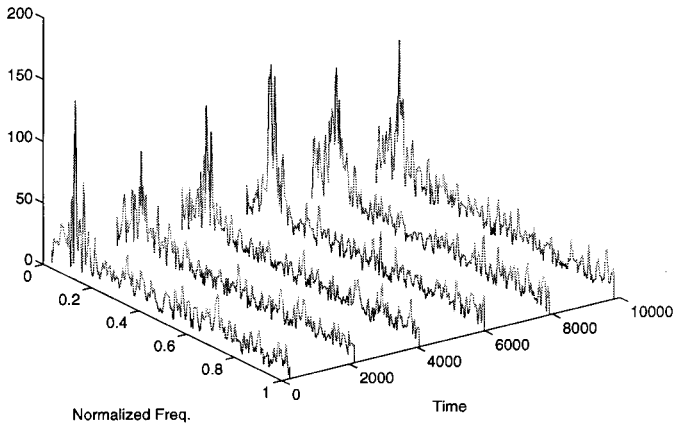

Fig. 1. Stationary AR1 process ($\alpha = 0.9$), 256 point Hanning windowed FFT.

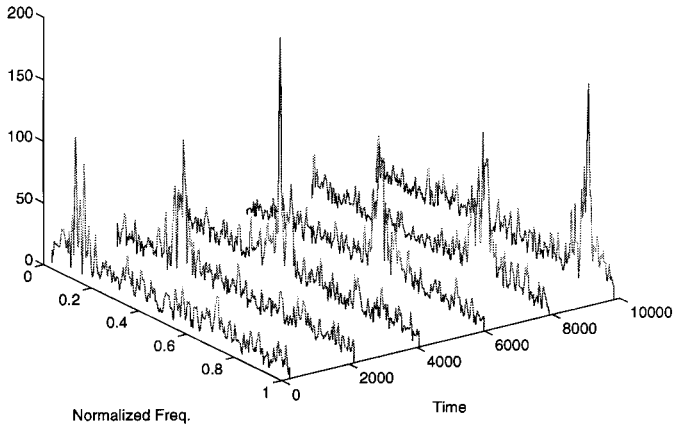

Fig. 2. Chirped AR1 process ($\alpha = 0.9$), 256 point Hanning windowed FFT.

Using the minimum prediction error (ξ_0) for the AR1 process from [13] in (45), the noise misadjustment is

$$\mathcal{M}_{k+1}^n = \frac{P_n\beta}{2}M\left[1+\rho(1-\alpha^2)\frac{(1-\alpha b)+(\alpha-b)b^{2M+1}}{(1-\alpha b)^2-(\alpha-b)^2b^{2M}}\right]. \tag{78}$$

Finally, the lag misadjustment can be obtained in closed form using (57) and is derived in Appendix D. Here, we show a more tractable form of $\mathcal{M}_{k+1}^{\Delta}$ in the limit as $M \to \infty$ for $(\alpha, b) > 0$[4]

$$\lim_{M\to\infty} \mathcal{M}_{k+1}^{\Delta} = P_n(\alpha-b)^2 \left[\frac{(1+b^2)}{(1-b^2)^3}+\rho\frac{b^2(1-\alpha^2)+2\alpha b(1-b^2)+(1-\alpha^2b^4)}{(1-\alpha b)^2(1-b^2)^3}\right]\frac{\psi^2}{\beta^2} \tag{79}$$

is the lag misadjustment normalized by ψ^2/β^2. This term illustrates the effects of various parameters on the lag misadjustment, notably, the lag misadjustment increases with the signal power and the ratio of the chirp rate over the adaptation constant (ψ/β). Fig. 3 plots the "normalized lag misadjustment" of the above expression $\kappa_{\max} = \mathrm{Lim}_{M\to\infty}\mathcal{M}_{k+1}^{\Delta}\beta^2/\psi^2$. It can be seen from Fig. 3 that the lag misadjustment increases

[4]Note in this case that the reflection term given by B_2 in the filter weights can be neglected as $B_2/B_1 \to 0$ for a finite bandwidth signal.

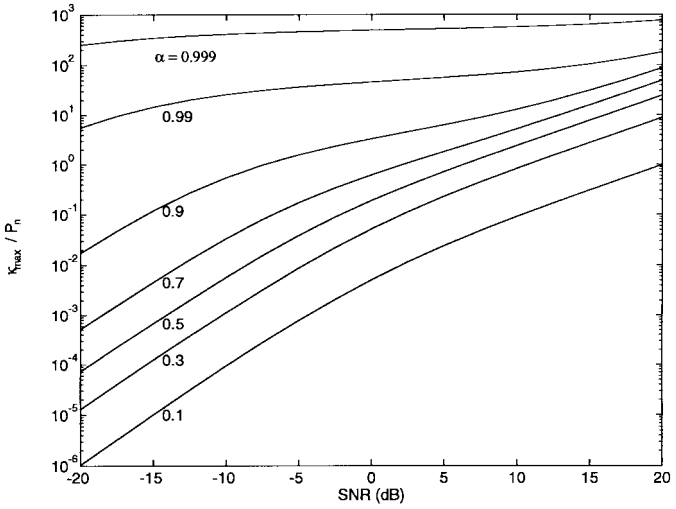

Fig. 3. Normalized lag misadjustment $\kappa_{\max}/P_n$ versus SNR for various AR1 correlation values (α).

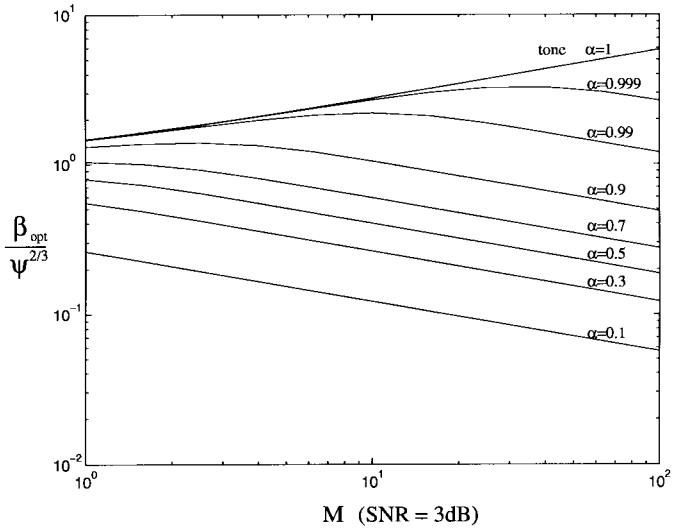

Fig. 4. Normalized adaptation constant $(\beta_{opt}/\psi^{2/3})$ versus filter length (M) for an AR1 process with correlation (α) at SNR = 3 dB. The top line plots the tone case.

with the SNR and decreases as the signal bandwidth increases. This is because with the decrease in correlation, both the magnitude of the optimum weights and the lag misadjustment (58) decreases. This result satisfies the intuitive notion that the lag misadjustment is zero when tracking a white (unpredictable) *signal* since the optimum filter is zero, and the signal is present at all frequencies. The main difference between this result and the deterministic chirp case is that as the number of filter taps increases, there is an upper bound on the lag error for finite bandwidth signals, whereas for the deterministic chirp, the lag error increases as M^2. This is because the magnitude of the weights for deterministic chirp do not decay, and the lag error increases without bound as M^2 in (57). In other respects, the performance with respect to $(P_n\psi^2/\beta^2)$ is the same, regardless of the signal bandwidth.

Fig. 4 plots the optimum adaptation constant normalized by the chirp rate $(\beta_{opt}/\psi^{2/3})$ for SNR = 3 dB at various filter

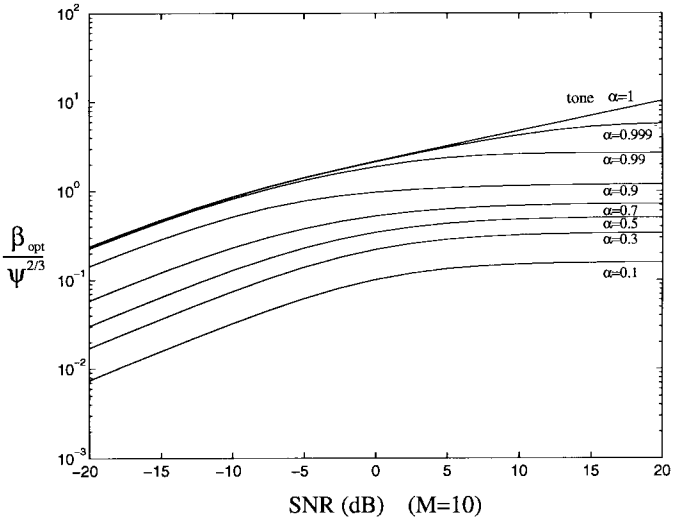

Fig. 5. Normalized adaptation constant $(\beta_{opt}/\psi^{2/3})$ versus SNR for an AR1 process with correlation (α) at $M = 10$. The top line plots the tone case.

lengths (M) and signal correlation (α). It can be seen that the adaptation constant increases with M. However, for the chirped nonzero bandwidth signals, β_{opt} reaches a maximum near $1/\alpha$, after which, additional increase in the filter length essentially requires reduction of the update size. For the chirped tone, β_{opt} increase with M.

Fig. 5 plots $(\beta_{opt}/\psi^{2/3})$ for $M = 10$ at various SNR's and signal correlations. It can be seen that the adaptation constant increases with both SNR and signal correlation (α).

Finally, Fig. 6 plots the normalized estimation error of the RLS algorithm using the optimum adaptation constant (β_{opt}) when the input is a chirped AR1 process with input SNR = 3 dB and chirped at $\psi = 5\pi 10^{-5}$. It can be seen that in addition to a β_{opt} for a given filter length, there is an optimum filter length that achieves the minimum prediction error. As compared with Fig. 4, the minimum error occurs before the optimum adaptation constant reaches a maximum. Note also that as the signal bandwidth decreases, the prediction error is more sensitive to the filter length.

VIII. Simulations

To demonstrate the validity of the analysis, namely, the existence of the optimum β_{opt} and the agreement between the theoretical to the experimental results, several simulations have been performed using the chirped AR1 process. The stationary and chirped signal was generated using (71) with $\psi = 0$ and $\psi = \psi_0$, respectively, with the same noise sequence $\{u_k\}$. This is then added to the white noise $\{n_k\}$ to give the input sequence for the stationary and chirped signal. A RLS filter was applied to both sequences, and the *misadjustment ratio* was calculated using ξ/ξ_0, where[5]

$$\xi = E|e(k)|^2. \tag{80}$$

[5]The ξ_0 used for normalization in the plots was measured using the *stationary* input sequence and the optimum Wiener filter computed from the data sequence. This is used instead of (17) to smooth the variations caused by the short run lengths that were chosen to prevent the spectrum from wrapping around.

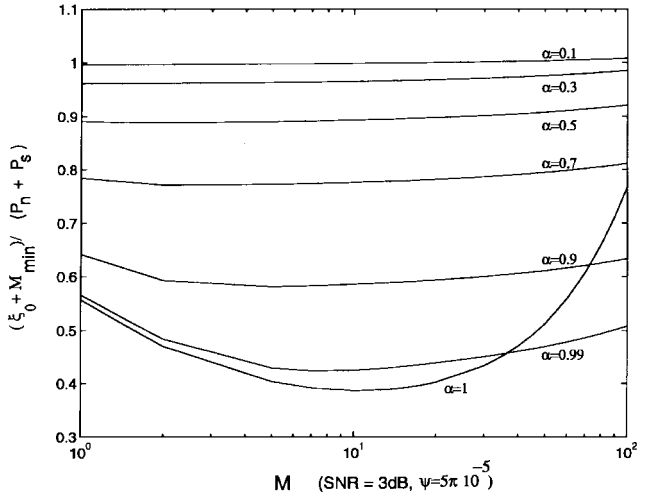

Fig. 6. The normalized RLS prediction error $(\xi_0+\mathcal{M}_{\min})/(P_n+P_s)$ using the optimum adaptation constant (β_{opt}) versus filter length (M) for an AR1 process with correlation (α) at SNR $=$ 3 dB.

TABLE I
SIMULATION PARAMETERS

β	$[\frac{1}{10},\ \frac{1}{5},\ \frac{1}{2},\ 1,\ 2,\ 5,\ 10]\beta_{opt}$
ρ	2, 32
α	0.5, 0.9, 0.99, 0.995
ω	0.2π
ψ	$[5,\ 0.5]\pi 10^{-5}$
M	3, 10

Simulations were performed with combinations of parameters shown in Table I. Since all results were qualitatively similar, the case $(M = 10, \rho = 2, \alpha = 0.9, \omega = 0.2\pi, \psi = 5 * 10^{-5}\pi)$ is used to illustrate the results. The weights were first initialized to the optimum weights, and the simulation was performed for 10 000 iterations. The value of β_{opt} can be obtained from Fig. 4 using $M = 10$ and using $\psi = 5 * 10^{-5}\pi$ in (65) to give $\beta_{opt} = 3.04 * 10^{-3}$.

The minimum recovery error, minimum estimation error, and output recovery SNR are $\eta^2 = 1.437$, $\xi_0 = 3.437$, and $\rho_0 = 2.783$. Fig. 8 plots the transfer function of the RLS filter. It can be seen that as β is decreased from $2\beta_{opt}$ to $\beta_{opt}/2$, the magnitude of lag filter increases. This introduces an increased lag in the overall RLS transfer function.

Fig. 7 plots the first two weights of the RLS filter over time for $\beta = (2, 1, 0.5)\beta_{opt}$. It can be seen that when $\beta \geq \beta_{opt}$, the filter easily tracks the optimum weights. The small mean lag here is covered by the weight fluctuations. As β is decreased, the weight fluctuation can be seen to decrease at the cost of increased lag. This illustrates the tracking speed versus estimation noise in the filter weights.

Finally, Fig. 9 plots the misadjustment of the RLS filter for both a stationary and a chirped AR1 signal, averaged over 10 simulation runs.[6] The symbols denote the simulation results, the vertical bars are the $\pm\sigma$ error bars, and the solid lines are the theoretical results. The effect of the adaptation parameter

[6]The theoretical noise misadjustment used in Figs. 9 and 10 is taken from (46), which is more accurate for large values of β.

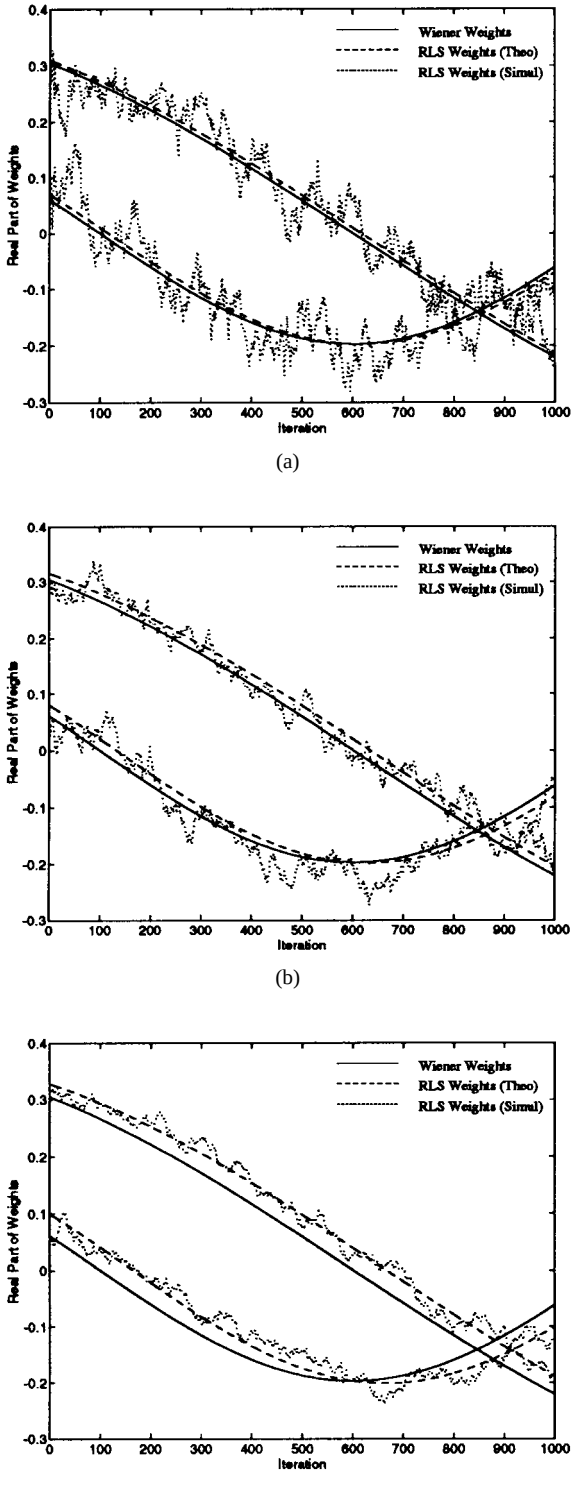

Fig. 7. Filter weights versus time for various β for chirped AR1 process.

(β) on the misadjustment is evident as β varied from β_{opt}. There are two main regions on the plots:

- When $\beta \geq \beta_{opt}$, the filter tracks the chirped signal. Here, the lag is negligible, and the error output is dominated by the noise misadjustment. Thus, from Fig. 9, the chirped and stationary results lie on top of one another.
- When $\beta < \beta_{opt}$, the filter is unable to track the input changes, and the output error caused by the lag misadjust-

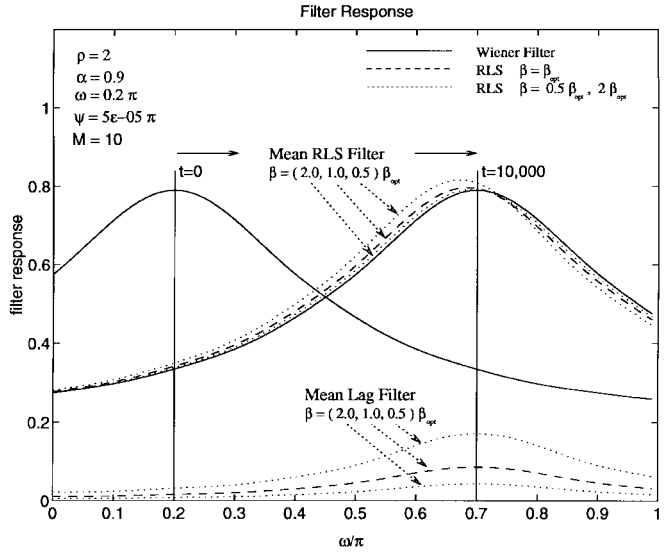

Fig. 8. Filter transfer function over time for a chirped AR1 process.

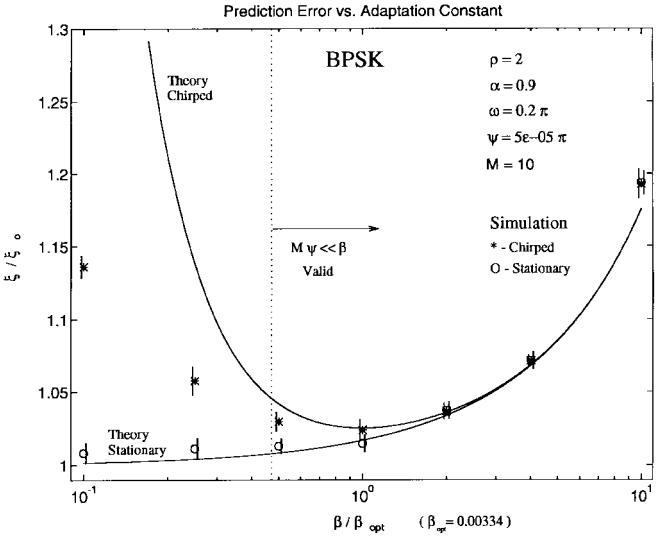

Fig. 10. Misadjustment ratio (ξ/ξ_0) versus adaptation constant (β) for a chirped BPSK signal.

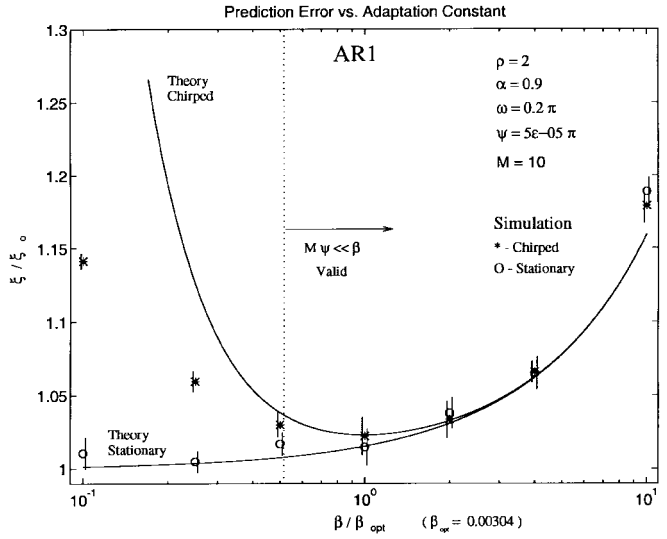

Fig. 9. Misadjustment ratio (ξ/ξ_0) versus adaptation constant (β) for a chirped AR1 process.

ment is evident in Fig. 9. From Fig. 9, as β is decreased, the error is seen to increase, whereas for the stationary case, the error decreases.

In all cases, the simulations were very close to the theoretical results near β_{opt}. Two points to note are that 1) when the adaptation parameter β becomes large, the simulation results tends to be larger than the theory for both the stationary and chirped signal, and 2) when β is too small and no longer satisfies the slow variation assumption $(M\psi \ll \beta)$, the actual misadjustment is smaller than this analysis predicts.

A. Communication Signals (BPSK)

One use of these results will be to track communication signals using adaptive filters. Here, a BPSK signal is used to demonstrate the applicability of these results.

$$s(k) = \sqrt{2P_s}b_{k/T}\cos\frac{\omega k + \psi k^2}{2} \tag{81}$$

where b_i is the binary (± 1) information sequence. When demodulated with an I and Q channel, the autocorrelation is of the form (6), and preceding results can be used to determine the optimum adaptation parameter. A BPSK signal with $1/T = (1-\alpha) = 0.1$ corresponding to the previous AR1 signal with $\alpha = 0.9$ is chosen. Using the same $(M,\ \rho,\ \omega,\ \psi)$ parameters as before, the optimum adaptation constant is $\beta_{opt} = 3.34{*}10^{-3}$. The minimum recovery error, minimum estimation error, and output recovery SNR are $\eta^2 = 0.845$, $\xi_0 = 2.845$, and $\rho_0 = 4.733$. Although in this example the recovery error powers are significantly different from those predicted by the AR1 model, the adaptation constant (β_{opt}) is very similar. The adaptation constant is slightly larger for the BPSK signal process because the BPSK signal correlation falls off linearly, whereas the AR1 decreases exponentially. This translates to an increased normalized lag (κ) for the BPSK signal and, thus, a larger adaptation constant. The recovery error powers predicted by the AR1 model of the BPSK signal improves as α increases $(\alpha \approx 0.99)$ [14]. The output misadjustment versus the β for the BPSK signal is plotted in Fig. 10. This plot shows the same behavior as the previous plot for the AR1 process.

IX. Conclusion

This paper studied the performance of the RLS algorithm for a generalized chirped signal by decomposing the filter into the Wiener, lag, and noise misadjustment filters. The optimum Wiener weights were derived for a *general* chirped signal and are shown to be a chirped version of the weights for the *stationary* signal. The filter spectrum essentially tracks the input spectrum. The lag misadjustment filter is shown to increase in magnitude as $1/\beta$ and is centered on the chirped signal. However, when added to the Wiener filter, the phases of the filter coefficients are shifted to produce a mean filter spectrum that lags the input signal.

The nonstationary weight model for the chirp is shown to be similar to the first order Markov model studied in [3], however, with a chirping forcing function. In this case, the updates sum

coherently to give a $1/\beta^2$ factor in the lag misadjustment rather than the $1/\beta$ factor in [3].

Expressions for the optimum adaptation constant (β_{opt}), which minimizes the mean squared output error (MSE), were derived for a general chirped signal and given analytically for the AR1 process. Furthermore, there is an optimum filter length (less than $1/\alpha$) that minimizes the MSE for a given chirp rate. Simulations were performed to demonstrate the validity of the analysis for both the chirped AR1 and chirped BPSK signals. For $\beta = \beta_{opt}$, the lag misadjustment is shown to be half the noise misadjustment, and hence, it is possible to optimize the filter for a maximum chirp rate and have approximately the same performance when the signal is chirped at a equal or slower rate.

Appendix A
Derivation of RLS Correlation Matrix Estimate $E[\mathbf{R}_k]$

The RLS estimate of the correlation matrix is

$$\begin{aligned} E[\mathbf{R}_k] &= \sum_{j=1}^{k} \lambda^{k-j} E[\overline{x}_j^* \overline{x}_j^T] \\ &= \frac{1-\lambda^k}{1-\lambda} P_n \mathbf{I} + \rho P_n \mathbf{R} \\ &\quad \odot \left[\sum_{j=1}^{k} \lambda^{k-j} \mathbf{V}^j \overline{\mathrm{D}}\, \overline{\mathrm{D}}^H \mathbf{V}^{*j} \right]. \end{aligned} \tag{A1}$$

The (p, q)th element of the matrix $\mathbf{V}^j \overline{\mathrm{D}}\, \overline{\mathrm{D}}^H \mathbf{V}^{*j}$ is given by

$$[\mathbf{V}^j \overline{\mathrm{D}}\, \overline{\mathrm{D}}^H \mathbf{V}^{*j}]_{p,q} = \Psi^{j(p-q)} \Omega^{p-q} \Psi^{-(p^2-q^2)/2}. \tag{A2}$$

It can be seen that each element in the summed matrix is the summation of a geometric series. Thus, defining

$$\begin{aligned} \mathbf{H}_j(\lambda) &: (\mathbf{H}_j)_{p,q} \\ &= \frac{\Psi^{j(p-q)} \Omega^{p-q} \Psi^{-(p^2-q^2)/2}}{\Psi^{(p-q)} - \lambda} \\ \mathbf{H}_j(\lambda) &= \beta^{-1} \mathbf{V}^j (\mathcal{C} \odot \overline{\mathrm{D}}\, \overline{\mathrm{D}}^H) \mathbf{V}^{*j} \end{aligned} \tag{A3}$$

where

$$\begin{aligned} \mathcal{C} &: (\mathcal{C})_{p,q} \\ &= \left[1 - \frac{1-\Psi^{(p-q)}}{\beta} \right]^{-1} \\ &\approx 1, \qquad M\psi \ll \beta \end{aligned} \tag{A4}$$

the RLS estimate of the correlation matrix can be written as

$$E[\mathbf{R}_j] = \frac{1-\lambda^j}{1-\lambda} P_n \mathbf{I} P_n \mathbf{R} \odot [\mathbf{H}_{j+1}(\lambda) - \lambda^j \mathbf{H}_1(\lambda)].$$

In the steady state, where $j = k \to \infty$, the λ^j term vanishes, and the correlation estimate simplifies to

$$E[\mathbf{R}_k] = \frac{P_n}{\beta} \mathbf{V}^{k+1} \mathcal{D}_{\mathcal{C}} \mathbf{V}^{*k+1} \tag{A5}$$

where

$$\mathcal{D}_{\mathcal{C}} = \mathbf{I} + \rho \mathcal{C} \odot [\mathbf{R} \odot (\overline{\mathrm{D}}\, \overline{\mathrm{D}}^H)]. \tag{A6}$$

It can be seen here that the chirped signal distorts the estimate of correlation matrix multiplicatively through the matrix $\mathcal{C}$. When the slow variations assumption hold ($M\psi \ll \beta$), the matrix $\mathcal{D}_{\mathcal{C}} \to \mathcal{D}$, and the RLS estimates of the correlation simplifies to

$$E[\mathbf{R}_k] \approx \frac{P_n}{\beta} \mathbf{V}^{k+1} \mathcal{D} \mathbf{V}^{*k+1} \tag{A7}$$

where $\mathcal{D} = \mathbf{I} + \rho \mathbf{R} \odot (\overline{\mathrm{D}}\, \overline{\mathrm{D}}^H)$, and

$$\mathbf{R}_k^{-1} \approx \frac{\beta}{P_n} \mathbf{V}^{k+1} \mathcal{D}^{-1} \mathbf{V}^{*(k+1)}. \tag{A8}$$

From above, even when the filter is able to track the input correlation, the RLS estimate of the correlation matrix is biased as compared with (10). However, for slow chirp rates, it is nearly identical.

Appendix B
Noise Misadjustment

Viewing $\mathbf{R}_k$ as deterministic, and $\overline{x}_n$ for $n \neq k+1$ independent of $\overline{x}_{k+1}$

$$\mathcal{M}_{k+1}^n = \xi_0 \sum_{n=1}^{k} \lambda^{2k-2n} \operatorname{Tr} \{E[\mathbf{R}_k^{-1} \overline{x}_{k+1}^* \overline{x}_{k+1}^T \mathbf{R}_k^{-1} \overline{x}_n^* \overline{x}_n^T]\}.$$

Recall that

$$\mathbf{\Phi}_j^x = E[\overline{x}_j^* \overline{x}_j^T] = P_n \mathbf{V}^j \mathcal{D} \mathbf{V}^{*j} \tag{B1}$$

where $\mathcal{D} = \mathbf{I} + \rho \mathbf{R} \odot (\overline{\mathrm{D}}\, \overline{\mathrm{D}})$.

Thus, using the quasideterministic property of $\mathbf{R}_k$

$$\mathcal{M}_{k+1}^n = \beta^2 \xi_0 \operatorname{Tr} \{\mathbf{V}^{k+1} \mathcal{D}^{-1} \mathbf{V}^{*(k+1)} v_k\}$$

where

$$v_k = \sum_{n=1}^{k} \lambda^{2k-2n} \mathbf{V}^n \mathcal{D} \mathbf{V}^{*n}.$$

The term v_k is similar to $E[\mathbf{R}_k]/P_n$ in (A1) with λ replaced by λ^2. Thus, for large k and $\beta \ll 1$, we have

$$v_k = \frac{1}{2\beta} \mathbf{V}^{k+1} \mathcal{D} \mathbf{V}^{*(k+1)} \tag{B2}$$

where the approximation $1 - \lambda^2 \approx 2\beta$ has been used, and

$$\mathcal{M}_{k+1}^n = \frac{\beta}{2} \operatorname{Tr}[I] \xi_0 = \frac{\beta}{2} M \xi_0. \tag{B3}$$

Appendix C
Mean Lag Misadjustment

Using $\mathbf{R}_j$ from (A5), the summation in Δ_k from (48) can be decomposed into

$$\begin{aligned} \Delta_k = &- P_n \mathbf{R}_k^{-1} \sum_{j=1}^{k} \lambda^{k-j} \\ &\cdot \left[\frac{1-\lambda^j}{1-\lambda} \mathbf{I} + \rho \mathbf{R} \odot (\mathbf{H}_{j+1} - \lambda^j \mathbf{H}_1) \right] \overline{T}_j \end{aligned} \tag{C1}$$

where

$$\overline{T}_j = \overline{W}_{j+1}^0 - \overline{W}_j^0, \tag{C2}$$

$$\overline{W}_j^0 = \mathbf{V}^j \mathbf{\Lambda} \overline{z} \tag{C3}$$

and $\overline{z} = \rho \mathcal{D}^{-1} (\overline{r} \odot \overline{\mathrm{D}}) = \overline{W}^0 \odot \overline{\mathrm{D}}$.

Expanding Δ_k into the constituent terms

$$\Delta_k = -P_n \mathbf{R}_k^{-1}[t_1 + t_2 + t_3 + t_4](\mathbf{V} - \mathbf{I})\overline{z} \tag{C4}$$

where

$$t_1 = \frac{1}{\beta}\sum_{j=1}^{k} \lambda^{k-j}\mathbf{V}^j,$$

$$t_2 = -\frac{\lambda^k}{\beta}\sum_{j=1}^{k} \mathbf{V}^j, \tag{C5}$$

$$t_3 = \rho\left[\mathbf{R} \odot \sum_{j=1}^{k} \lambda^{k-j}\mathbf{H}_{j+1}\mathbf{V}^j\right]$$

$$= \rho\left[\mathbf{R} \odot \sum_{j=1}^{k} \lambda^{k-j}\mathbf{V}^j\beta^{-1}\mathbf{V}(\mathcal{C} \odot \overline{\mathrm{D}}\,\overline{\mathrm{D}}^H)\mathbf{V}^*\right]$$

$$= \rho\left[\sum_{j=1}^{k} \lambda^{k-j}\mathbf{V}^j\right](\mathbf{R} \odot \mathbf{H}_1), \tag{C6}$$

and

$$t_4 = -\rho\lambda^k\left[(\mathbf{R} \odot \mathbf{H}_1)\sum_{j=1}^{k} \mathbf{V}^j\right]. \tag{C7}$$

For $k \gg 1$, $\lambda^k \to 0$, the terms (t_2, t_4) can be neglected since the sum

$$t_5 = \sum_{j=1}^{k} \mathbf{V}^j$$

$$= \mathbf{V}(\mathbf{I} - \mathbf{V}^k)(\mathbf{I} - \mathbf{V})^{-1} \tag{C8}$$

is bounded. The remaining terms t_1 and t_3 are dependent on the following sum (t_6), where

$$t_6 = \sum_{j=1}^{k} \lambda^{k-j}\mathbf{V}^j$$

$$= \mathbf{V}^k(\mathbf{I} - \lambda^k\mathbf{V}^{-k})(\mathbf{I} - \lambda\mathbf{V}^{-1})^{-1}$$

$$\approx \mathbf{V}^{k+1}(\mathbf{V} - \lambda\mathbf{I})^{-1}, \qquad k \gg 1. \tag{C9}$$

Thus, substituting t_6 in (t_1, t_3), Δ_k becomes

$$\Delta(k) = -P_n\mathbf{R}_k^{-1}\frac{\mathbf{V}^{k+1}}{\beta}(\mathbf{V} - \lambda\mathbf{I})^{-1} \cdot (\mathbf{I} + \rho\beta\mathbf{R} \odot \mathbf{H}_1)(\mathbf{V} - \mathbf{I})\overline{z}. \tag{C10}$$

Appendix D
Derivation of κ for AR1 Process

For slow chirp rates $\psi \ll 1$,

$$\kappa \approx \frac{(\mathbf{\Lambda}\overline{W}^0)^H\mathbf{\Phi}^x(\mathbf{\Lambda}\overline{W}^0)}{\psi^2}, \qquad \psi \ll 1 \tag{D1}$$

with

$$(\mathbf{\Lambda})_{m,n} \approx \sqrt{-1}(m\psi)\delta_{m,n}. \tag{D2}$$

This approximation is extremely good for $m\psi \leq 0.001$ and in these cases, the exact evaluation of $\mathcal{M}^{\Delta}$ using the exact and approximate κ produced very little difference.

The correlation matrix of an AR1 process embedded in white noise and the Wiener weights for the one-step prediction filter are

$$(\Phi_x)_{m,n} = P_n(\delta_{m,n} + \rho\alpha^{|m-n|}) \tag{D3}$$

and

$$(\overline{W}^0)_l = B_1 b^l + B_2 b^{M-l}, \qquad l = 1, \cdots, M. \tag{D4}$$

Thus, κ can be written as

$$\kappa = P_n\sum_{m,n=1}^{M} mn(\overline{W}^0)_m^*(\overline{W}^0)_n\alpha^{|m-n|}. \tag{D5}$$

We now define several summations:

$$S_1(q) = \sum_{k=1}^{M} kq^k \tag{D6}$$

$$S_2(q) = \sum_{k=1}^{M} k^2q^k \tag{D7}$$

$$SS(a, b_1, b_2) = \sum_{i,j=1}^{M} ija^{|i-j|}b_1^i b_2^j \tag{D8}$$

which can be expressed analytically.

Using S_1, S_2, and SS with (D4) in (D3), κ can be written as

$$\kappa = P_n\Bigg\{B_1^2[S_2(b^2) + \rho SS(\alpha, b, b)] + B_2^2b^{2M}\left[S_2\left(\frac{1}{b^2}\right) + \rho SS\left(\alpha, \frac{1}{b}, \frac{1}{b}\right)\right] + 2B_1B_2b^M \cdot \left[\underbrace{\frac{M(M+2)(2M+1)}{6}}_{S_2(1)} + \rho SS\left(\alpha, b, \frac{1}{b}\right)\right]\Bigg\}. \tag{D9}$$

The appropriate limits can be taken on b, B_1, B_2, S_1, S_2, and SS for the limiting case $\alpha \to 1$, and use of the large SNR assumption used in [7] ($M\rho >> 1$) gives results that correspond to the deterministic chirp result.

$$\lim_{\alpha\to 0}\kappa = \frac{P_n}{4}(M+1)^2\rho. \tag{D10}$$

Appendix E
$\mathbf{R}_k$ is Quasi-Deterministic

The variance of the correlation matrix estimate is

$$\mathbf{B}_k = E[(\mathbf{R}_k - E[\mathbf{R}_k])^2] \tag{E1}$$

where

$$\mathbf{R}_k - E[\mathbf{R}_k] = \sum_{l=1}^{k} \lambda^{k-l}[\overline{x}_l^*\overline{x}_l^T - \mathbf{\Phi}_l^x].$$

Expanding $\mathbf{B}_k$

$$\mathbf{B}_k = \sum_{i,m=1}^{k} \lambda^{2k-i-m}\{E[\overline{x}_i^*\overline{x}_i^T\overline{x}_m^*\overline{x}_m^T] - \mathbf{\Phi}_i^x\mathbf{\Phi}_m^x\} \tag{E2}$$

where

$$E[\overline{x}_i^*\overline{x}_i^T\overline{x}_m^*\overline{x}_m^T] = \mathbf{\Phi}_i\mathbf{\Phi}_m + MP_n^2(1+\rho)\mathbf{V}^i\mathcal{D}\mathbf{V}^{*i}\delta_{i,m} \tag{E3}$$

is derived in Appendix G.

Utilizing the assumption X_i and X_m are independent

$$\mathbf{B}_k = MP_n^2(1+\rho)\sum_{i=1}^{k}\lambda^{2k-2i}\mathbf{V}^i\mathcal{D}\mathbf{V}^{*i}. \tag{E4}$$

This is similar to the RLS correlation estimate (A1) with different parameters, thus giving

$$\mathbf{B}_k \approx \frac{P_n^2}{2\beta}M(1+\rho)\mathbf{V}^{k+1}\mathcal{D}\mathbf{V}^{*k+1}. \tag{E5}$$

The square of the correlation matrix is

$$E[\mathbf{R}_k]^2 = \mathbf{V}^{k+1}\left[\frac{P_n^2}{\beta^2}\mathcal{D}^2\right]\mathbf{V}^{*k+1}. \tag{E6}$$

Thus, for the quasideterministic property of the correlation matrix to hold $\mathbf{B}_k \ll E[\mathbf{R}_k]^2$, the following inequality must be satisfied

$$\beta M(1+\rho)\mathcal{D} \ll 2\mathcal{D}^2. \tag{E7}$$

The magnitude of the above matrices can be measured by the trace to give

$$\beta M^2(1+\rho)^2 \ll 2M(1+\rho)^2. \tag{E8}$$

Thus, the above inequality and the quasideterministic property of $\mathbf{R}_k$ is satisfied when

$$\beta M \ll 2. \tag{E9}$$

This is the same result as found in [7] for the chirp case. However, for our model, this constraint is slightly tighter since the quasideterministic property for the chirp must satisfy the inequality

$$\beta[M(1+\rho)+\rho] \ll 2[1+\rho(2+\rho M)]. \tag{E10}$$

Appendix F
Derivation of $E[\overline{x}_i^*\overline{x}_i^T\overline{x}_m^*\overline{x}_m^T]$

For zero mean Gaussian variables, it can be shown that

$$E[\overline{x}_i^*\overline{x}_i^T\overline{x}_m^*\overline{x}_m^T] = E[\overline{x}_i^*\overline{x}_i^T]E[\overline{x}_m^*\overline{x}_m^T] + E[\overline{x}_i^*\overline{x}_m^H]E[\overline{x}_i\overline{x}_m^T] + E[\overline{x}_i^T\overline{x}_m^*]E[\overline{x}_i^*\overline{x}_m^T]. \tag{F1}$$

The first term of (F1) is the input correlation at time i multiplied by the correlation at time k.

The second term evaluates to zero since the input is composed of circularly complex Gaussian random variables, and the nonconjugated terms evaluate to zero.

Using the independence of the signal and noise, the third term of (F1) can be expanded as

$$E[\overline{x}_i^T\overline{x}_m^*] = E[\overline{n}_i^T\overline{n}_m^*] + E[\overline{s}_i^T\overline{s}_m^*]. \tag{F2}$$

Using the assumption that *successive input vectors are independent*, we can write

$$E[\overline{n}_i^T\overline{n}_m^*] = MP_n\delta_{i,m}$$

and

$$E[\overline{s}_i^T\overline{s}_m^*] = MP_s\delta_{i,m}. \tag{F3}$$

Similarly, the signal and noise covariance matrices are

$$E[\overline{s}_i^*\overline{s}_m^T] = \mathbf{\Phi}_i^s\delta_{i,m}.$$

and

$$E[\overline{n}_i^*\overline{n}_m^T] = P_n\mathbf{I}. \tag{F4}$$

Finally, combining the various terms gives the desired result:

$$\begin{aligned}E[\overline{x}_i^*\overline{x}_i^T\overline{x}_m^*\overline{x}_m^T] &= \mathbf{\Phi}_i^x\mathbf{\Phi}_m^x + MP_n(1+\rho)(P_n\mathbf{I}+\Phi_i^s)\delta_{i,m}\\ &= \mathbf{\Phi}_i^x\mathbf{\Phi}_m^x + MP_n^2(1+\rho)\mathbf{V}^i\mathcal{D}\mathbf{V}^{*i}\delta_{i,m}\end{aligned} \tag{F5}$$

where $\mathcal{D}$ is defined in (11).

Appendix G
Derivation of Identities used in Section III

Given $\mathbf{L}$, which is a diagonal matrix, $\mathbf{R}$, which is a matrix, $\overline{r}$, which is a vector, and $\overline{c}$, which has elements $|\overline{c}_k| = 1$, then

$$[\mathbf{L}+\mathbf{R}\odot(\overline{c}\overline{c}^H)](\overline{r}\odot\overline{c}) = [(\mathbf{L}+\mathbf{R})\overline{r}]\odot\overline{c} \tag{G1}$$

$$[\mathbf{L}+\mathbf{R}\odot(\overline{c}\overline{c}^H)]^{-1}(\overline{r}\odot\overline{c}) = [(\mathbf{L}+\mathbf{R})^{-1}\overline{r}]\odot\overline{c}. \tag{G2}$$

The first equality (G1)

$$[\mathbf{\Lambda}+\mathbf{R}\odot(\overline{c}\overline{c}^H)](\overline{r}\odot\overline{c}) = [(\mathbf{\Lambda}+\mathbf{R})\overline{r}]\odot\overline{c} \tag{G3}$$

is easily verified by writing the elements of the matrices.

The second equality G2

$$[\mathbf{L}+\mathbf{R}\odot(\overline{c}\overline{c}^H)]^{-1}(\overline{r}\odot\overline{c}) = [(\mathbf{L}+\mathbf{R})^{-1}\overline{r}]\odot\overline{c}$$

can be derived by expanding $\mathbf{R}$ in terms of its singular value decomposition ($\mathbf{R}=\mathbf{ULV}$) and noting that $\mathbf{R}\odot(\overline{c}\ \overline{c}^H) = [\mathbf{U}\odot(\overline{c}\ \overline{o}^H)]\mathbf{L}[\mathbf{V}\odot(\overline{c}\ \overline{o}^H)]^H$, where $\overline{o} = [1,\cdots,1]^T$. The form above is obtained after some simplification.

Acknowledgment

The authors would like the acknowledge the pioneering works of O. Macchi and N. J. Bershad for the analysis of RLS performance with noise-corrupted deterministic chirp input and Masry for the results on the AR1 process for interference suppression. They would also like to thank the many detailed suggestions by the reviewers that have improved the readability of the paper.

References

[1] S. Haykin, *Adaptive Filter Theory*, 3rd ed. Englewwod Cliffs, NJ: Prentice-Hall, 1996.
[2] B. Widrow, J. McCool, M. Larimore, and C. Johnson, "Stationary and nonstationary learning characteristics of the LMS adaptive filter," *Proc. IEEE*, vol. 64, pp. 1151–1162, Aug. 1976.
[3] E. Eleftheriou and D. D. Falconer, "Tracking properties and steady state performance of RLS adaptive filter algorithms," *IEEE Trans. Acoust., Speech, Signal Processing*, vol. ASSP-34, pp. 1097–1110, Dec. 1986.
[4] O. Macchi, "Optimization of adaptive identification for time-varying filters," *IEEE Trans. Automat. Contr.*, vol. AC-31, pp. 283–287, Mar. 1986.
[5] J. Lin, J. G. Proakis, F. Lin, and H. Lev-Ari, "Optimal tracking of time-varying channels: A frequency domain approach for known and new algorithms," *IEEE J. Selected Areas Commun.*, vol. 12, pp. 141–153, Jan. 1995.
[6] S. Haykin, A. Sayed, J. Zeidler, P. Wei, and P. Yee, "Tracking of time-varying systems," *IEEE Trans. Signal Processing*, in press.
[7] O. Macchi and N. J. Bershad, "Adaptive recovery of a chirped sinusoid in noise, 1. Performance of the RLS algorithm," *IEEE Trans. Acoust., Speech, Signal Processing*, vol. 39, pp. 583–594, Mar. 1991.
[8] N. Bershad and O. M. Macchi, "Adaptive recovery of a chirped sinusoid in noise, 2. Performance of the LMS algorithm," *IEEE Trans. Acoust., Speech, Signal Processing*, vol. 39, pp. 595–602, Mar. 1991.
[9] O. Macchi, N. Bershad, and M. Mboup, "Steady-state superiority of LMS over LS for time-varying line enhancer in noisy environment," *Proc. Inst. Elect. Eng.*, pt. F, vol. 138, pp. 354–360, Aug. 1991.

[10] K. C. Chew, T. Soni, J. R. Zeidler, and W. H. Ku, "Tracking model of an adaptive lattice filter for a linear chirp FM signal in noise," *IEEE Trans. Signal Processing*, vol. 42, pp. 1939–1951, Aug. 1994.
[11] T. Soni, J. R. Zeidler, and W. H. Ku, "Behavior of the partial correlation coefficients of a least squares lattice filter in the presence of a nonstationary chirp input," *IEEE Trans. Signal Processing*, vol. 43, pp. 852–63, Apr. 1995.
[12] P. C. Wei, "Performance evaluation of adaptive filtering algorithms for the mobile communication environment," Ph.D. dissertation, University of California, San Diego, La Jolla, 1995.
[13] E. Masry, "Closed form result for the rejection of narrow-band interference in PN spread spectrum systems—Part I: Linear prediction filters," *IEEE Trans. Commun.*, vol. COM-32, pp. 888–896, Aug. 1984.
[14] P. C. Wei, J. R. Zeidler, and W. H. Ku, "Adaptive interference suppression for CDMA overlay systems," *IEEE J. Selected Areas Commun.*, Special Issue on Intelligent Signal Processing in Communications—Part I, vol. 12, pp. 1510–1523, Dec. 1994.

Paul C. Wei (M'95) received the B.S. degree in electrical engineering from the University of California, Los Angeles, in 1989. He received the M.S. and Ph.D. degrees in electrical engineering from the University of California, San Diego, in 1991 and 1995, respectively.

He is currently working at the LSI Logic Wireless Design Center, Carlsbad, CA. He worked as an intern at the GM Technical Center, Warren, MI, during the summers of 1988 to 1990. From 1991 to 1995, he was a research assistant at the Industry/University Cooperative Research Center on Ultra High Speed Integrated Circuits and Systems, University of California, San Diego. He also worked part time at Hughes Network Systems, San Diego, CA, during the last year of his graduate work. His research interests include signal and image processing algorithms, applications of signal processing techniques to broadband communications, and performance of adaptive algorithms in high-speed hardware implementations.

James R. Zeidler (F'95) received the Ph.D. degree in physics from the University of Nebraska, Lincoln, in 1972.

He has worked at the Naval Command Control and Ocean Surveillance Center, RDT&E Division, San Diego, CA, since 1974, where he has done fundamental research and technology development on sonar and communications signal processing, image processing, and electronic devices. He has also been adjunct professor in the Department of Electrical and Computer Engineering, University of California, San Diego, since 1988.

Dr. Zeidler was an Associate Editor of the IEEE TRANSACTIONS ON SIGNAL PROCESSING. He received the award for best unclassified paper at the *IEEE MILCOM'95*.

Walter H. Ku (M'91) received the B.S. degree (with honors) from the Moore School of Electrical Engineering, University of Pennsylvania, Philadelphia, and the M.S. and Ph.D. degrees from the Polytechnic Institute, Brooklyn, NY.

In 1977, he was the first occupant of the Naval Electronic Systems Command (NAVELEX) Research Chair Professorship at the Naval Postgraduate School, Monterey, CA. As the NAVELEX Research Chair holder, he was an Expert Consultant to NAVELEX (now SPAWAR), Naval Research Laboratory (NRL), and OUSDRE. He has served over the years as a Consultant to the Department of Defense (DDR&E and ARPA) on the VHSIC and various GaAs monolithic integrated circuits programs, including the first DARPA-funded C- and X-band space-based radar modules, Air Force RADC, Griffith AFB, Rome, NY, and industrial laboratories. Since September 1985, he has been Professor of Electrical and Computer Engineering at the University of California, San Diego (UCSD), La Jolla, and is the Founding Director of the NSF I/UC Research Center on Ultra-High Speed Integrated Circuits and Systems (ICAS). He is also the Principal Investigator of a new five-year grant from DDR&E Focused Research Initiative (FRI) on Broadband Wireless Multimedia (BWM) Communications Systems. This FRI program was awarded in January 1995 and is a consortium lead by UCSD with Advanced Digital Technology (ADT), Hughes, Raytheon, Rockwell, and TRW as team members.

Dr. Ku is a member of Eta Kappa Nu, Tau Beta Pi, Sigma Tau, Phi Tau Phu, and Sigma Xi.